MOLECULAR AND CELLULAR BIOLOGY
2024, VOL. 44, NO. 9, 345–357
https://doi.org/10.1080/10985549.2024.2384600

The Ribosome Assembly Factor LSG1 Interacts with Vesicle-Associated Membrane Protein-Associated Proteins (VAPs)

Putri Sutjita[a], Sharmishtha Musalgaonkar[b*], Jeffrey Recchia-Rife[b#], Lisa Huang[b‡], Blerta Xhemalce[b], and Arlen W. Johnson[b]

[a]Interdisciplinary Life Sciences Graduate Program, The University of Texas at Austin, Austin, Texas, USA; [b]Department of Molecular Biosciences, The University of Texas at Austin, Austin, Texas, USA

ABSTRACT

LSG1 is a conserved GTPase involved in ribosome assembly. It is required for the eviction of the nuclear export adapter NMD3 from the pre-60S subunit in the cytoplasm. In human cells, LSG1 has also been shown to interact with vesicle-associated membrane protein-associated proteins (VAPs) that are found primarily on the endoplasmic reticulum. VAPs interact with a large host of proteins which contain FFAT motifs (two phenylalanines (FF) in an acidic tract) and are involved in many cellular functions including membrane traffic and regulation of lipid transport. Here, we show that human LSG1 binds to VAPs via a noncanonical FFAT-like motif. Deletion of this motif specifically disrupts the localization of LSG1 to the ER, without perturbing LSG1-dependent recycling of NMD3 *in cells* or modulation of LSG1 GTPase activity *in vitro*.

ARTICLE HISTORY
Received 29 February 2024
Revised 18 July 2024
Accepted 19 July 2024

KEYWORDS
Ribosome biogenesis; LSG1; VAP; vesicle-associated membrane protein-associated protein

Introduction

The assembly of ribosomes in eukaryotic cells is a complex and conserved pathway, requiring more than 200 transacting factors. Much of ribosome assembly is accomplished in the nucleolus, where the ribosomal DNAs are transcribed, and the resulting ribosomal RNAs (rRNAs) are modified, processed and assembled with ribosomal proteins (rproteins) into preribosomal particles.[1–4] However, the subunits that are exported to the cytoplasm lack critical ribosomal proteins and require additional assembly events before they are functional.[5–12] These include addition of the P-stalk, which allows the ribosome to recruit and engage translational GTPases, and the insertion of the ribosomal protein RPL10 (uL16) which completes the peptidyl transferase center.[5,10,13,14] In addition, pre-60S subunits entering the cytoplasm contain an entourage of factors that promote export as well as factors that prevent premature engagement with ligands of translation.[5,8,10,15] These factors must be released from the subunit before it can engage in translation. Among these factors, the nuclear export adapter NMD3 occupies the P and E sites, where it blocks binding of tRNAs[9,11] and promotes export by recruiting the nuclear export receptor CRM1 via a C-terminal leucine-rich nuclear export sequence.[16–18] The events of cytoplasmic maturation can be ordered into a hierarchical pathway[19] and recent structural studies have provided extensive mechanistic insight into the pathway of cytoplasmic maturation.[5–11]

LSG1 is a highly conserved protein involved in late stages of 60S maturation. In yeast, its GTPase is required for the release of the nuclear export adapter, NMD3.[20] Temperature-sensitive mutations or deletion of *LSG1* in yeast result in reduced levels of free 60S and the retention of NMD3 on pre-60S subunits.[20,21] In contrast to classical GTPases, the G-motifs comprising the GTPase domain of LSG1 are circularly permuted such that the G4 and G5 motifs precede the G1, G2, and G3 motifs.[22] Although circularly permuted, the arrangement of the domains maintains an overall structure similar to active sites seen in classical GTPases. We have shown previously that activation of the GTPase activity of yeast Lsg1 requires the presence of both 60S subunits and Nmd3.[11] A cryo-EM structure of Lsg1 bound to 60S revealed that Lsg1 binds to the inter-subunit surface of pre-60S particles where the rRNA helix 69 (H69)[11] positions Switch I of the GTPase center of Lsg1. We and others have proposed that Lsg1 couples the release of Nmd3 to the completion of the peptidyl transferase center of the ribosome by insertion of the ribosomal protein uL16.[5,20]

In human cells, the GTPase activity of LSG1 is also necessary for recycling NMD3 from 60S subunits.[23] Human LSG1 comprises 658 amino acids and contains an extended unstructured loop (aas 254–324) that is not conserved in

CONTACT Arlen W. Johnson arlen@utexas.edu
*Present address: SalioGen Therapeutics, Lexington, Massachusetts.
#Present address: Indiana University School of Medicine.
‡Present address: University of Texas MD Anderson Cancer Center.

yeast.[24] Unlike yeast Lsg1 that predominantly localizes to the cytoplasm, human LSG1 localizes to the nucleus (in Cajal bodies) and the cytoplasm (specifically the endoplasmic reticulum) at steady state.[23,24] It is not clear whether human LSG1 loads onto pre-60S in the nucleus or in the cytoplasm. Intriguingly, previous work from the Kutay lab identified the endoplasmic reticulum (ER)-localized vesicle-associated membrane protein-associated proteins (VAPA and VAPB, VAPs) as novel LSG1 interactors.[25] LSG1 and VAP interaction has also been detected in several large-scale proteomic screens.[26–28] The yeast homologs of VAP, Scs2 and Scs22, however, are not known to interact with yeast Lsg1.[29,30]

VAPs are highly conserved proteins found on the cytoplasmic face of the ER and are involved in many cellular processes such as membrane trafficking and lipid transport regulation.[31,32] VAPs interact with numerous proteins and interactions with proteins containing FFAT motifs (two phenylalanines in an acidic tract) are the best characterized.[31–33] The characteristic FFAT motif, which is found in many lipid transfer proteins, consists of a stretch of seven amino acids with six defined residues: E^1-F^2-F^3-D^4-A^5-X^6-E,[7] where "X" is any amino acid.[32,33] Residues immediately surrounding the motif contain multiple acidic, but very few basic, amino acids.[33] Proteins with accessible FFAT motifs are capable of binding VAPs which localizes them to the ER.[33,34] Although a known VAP interactor, LSG1 does not have a canonical FFAT motif. In this work, we map the LSG1 and VAP interaction surfaces. We then generate an LSG1 mutant that is defective for interaction with VAPs and show that this mutant complements the known function of LSG1 to promote the nuclear recycling on NMD3.

Results

LSG1 interacts with VAPs via an FFAT-like domain

Human LSG1 is a circularly permuted (cp) GTPase of 658 amino acids, in which the G1 through G3 motifs follow the G4 and G5 motifs (Figure 1A). Although cpGTPases are found from bacteria through eukaryotes and are dedicated to ribosome biogenesis,[24,35] the LSG1 family is found only in eukaryotes.[24] To verify the reported interaction between LSG1 and VAP[25] with the goal of determining the functional importance of this interaction, we utilized a yeast two hybrid assay to map the interactions surfaces between LSG1 and VAPA (Figure 1B and E to G). LSG1 was fused to the DNA binding domain of Gal4 (BD) and the soluble MSP and coiled-coil domains of VAPA were fused to the transcriptional activation domain of Gal4 (AD). Co-expression of BD-LSG1 and AD-VAPA supported growth on media lacking histidine, indicating physical interaction (Figure 1B, top row). Because LSG1 lacks an obvious canonical FFAT motif for binding to VAP, we generated a series of nested N-terminal and C-terminal deletions (Figure 1A and B). This deletion analysis showed that the N-terminal residues 1 to 254 and the C-terminal residues 324 to 658 of LSG1 were dispensable for VAPA interaction, suggesting that the region spanning amino acids (aas) 254–324 of LSG1 is responsible for VAPA binding. Deleting aas 254–324 of LSG1 abolished its interaction with VAPA, while expressing only aas 254–324 maintained VAPA interaction (Figure 1B, bottom). These results indicate that aas 254–324 of LSG1 are both necessary, and sufficient for VAPA interaction.

Amino acids 254–324 of LSG1 occur within a linker region between the G5 and G1 GTPase motifs. We previously determined the structure, using cryo-electron microscopy, of yeast Lsg1 bound to the 60S ribosomal subunit.[10,11] While the G motifs were well-resolved in those structures, the linker between the G5 and G1 motifs was not. In the human LSG1 protein, the linker is elaborated into a more extensive loop than that found in yeast Lsg1 (Figure 1C and D). Similarly, aas 253–324 were not resolved in a structure of human pre-60S containing LSG1.[7] Nevertheless, the structures indicate that the linker would be on the solvent side of LSG1, projecting away from the 60S subunit (Figure 1D). Thus, LSG1 binding to 60S is not necessarily mutually exclusive with binding to VAP. To better define the amino acids of LSG1 responsible for VAPA binding, we separately deleted the first half (Δ254–291) and second half (Δ292–324) of the linker in our yeast two-hybrid system. Deletion of amino acids 292–324, but not 254–291 resulted in loss of interaction with VAPA (Figure 1E). Alanine scanning mutagenesis across amino acids 292–324 showed that mutating amino acids 316–319 and 320–324 to alanine resulted in weakened VAPA interaction (Figure 1F). Although this region does not harbor a canonical FFAT motif, the sequence DWQTCSE (aas 317–323), which contains a tryptophan bracketed by acidic residues, is reminiscent of a FFAT motif, EFFDAxE (where x is any amino acid).[33,36] In particular, the DWQTCSE motif is preceded by a highly acidic tract (Figure 1E). The DWQTCSE sequence is well conserved among vertebrates, but not in lower eukaryotes (Figure 1E). Mutating DWQTCSE and the residues immediately before and after the motif to a stretch of nine alanines (LSG1-9Ala) significantly reduced but did not completely abolish VAP interaction (Figure 1G). The sequence EYEDCPE at residues 306–312 was identified as a potential FFAT-like motif within LSG1.[32] Although, our alanine scanning mutagenesis did not detect any defect in yeast two hybrid interaction when portions of the EYEDCPE sequence were mutated (Figure 1F), we decided to make an alanine-substituted mutant of this motif, both in combination with the alanine-substituted DWQTCSE mutant (LSG1-7Ala-9Ala) and alone (LSG1-7Ala) (Figure 1G). The double mutant lost all detectable binding to VAP, judged by yeast two hybrid, whereas the single alanine-substituted EYEDCPE mutant showed no loss of interaction. These results suggest that the DWQTCSE sequence is the primary VAP binding motif, while the EYEDCPE sequence is redundant with the DWQTCSE FFAT-like motif. Because the 9Ala mutation did not fully disrupt VAP interaction, we used the LSG1-Δ292–324 mutant, in which both VAP interaction motifs are deleted, in all subsequent work.

VAPs are highly conserved in eukaryotes with yeast Scs2 and Scs22 encoding VAP homologs. Because the mode of interaction with VAPs via FFAT or FFAT-like motifs is conserved, we tested if human LSG1 could interact with yeast VAPs. Indeed, human LSG1 but not yeast Lsg1 interacted with yeast Scs2, assayed by yeast two-hybrid (Figure 1H), consistent with yeast Lsg1 apparently lacking any FFAT-like

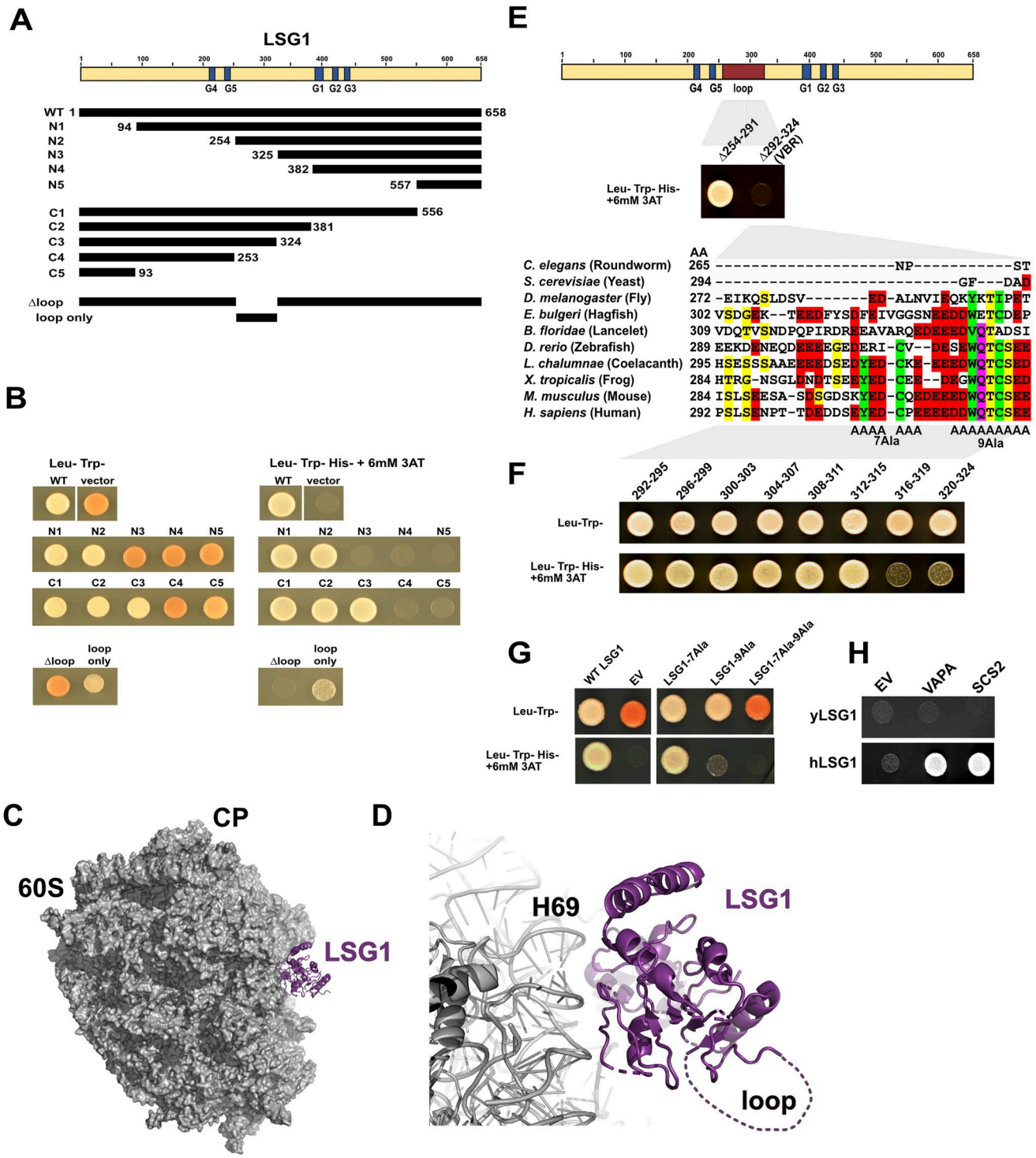

Figure 1. The VAP interaction domain of LSG1 is within an unstructured loop between the G5 and G1 motifs of LSG1. (A) Cartoon showing LSG1 with G motifs highlighted in blue and LSG1 deletion mutants. (B) Assay for 2-hybrid interaction between LSG1 constructs and the soluble domains of VAPA. Strains containing the indicated constructs were spotted onto Leu-Trp- media and Leu-Trp-His- media supplemented with 6 mM 3-Amino-1,2,4-triazole (3AT) as indicated. Growth on His- media with 3AT indicates interaction. Interaction also drives expression of the *ADE3* reporter, yielding white as opposed to red colony phenotype. (C) Human LSG1 (purple) on pre-60S (gray) (PDB 6LSR). (D) LSG1 on pre-60S zoomed, showing the expected position of the loop containing the VAP binding region facing away from the ribosome. (E) VAPA binds within the second half of the unstructured loop of LSG1. Multiple protein sequence alignment of LSG1 from the indicated organisms focusing on the VAP Binding Region of LSG1. Highlighting of residues is based on amino acid property: yellow, small nonpolar; green, hydrophobic; magenta, polar; red, negatively charged; blue, positively charged. (F) Yeast 2-hybrid interaction between alanine scanning mutants and the soluble domains of VAPA. (G) Yeast 2-hybrid interaction assay between LSG1 constructs and the soluble domains of VAPA. 7Ala is the EYEDCPE sequence mutated to seven alanines and 9Ala is the DDWQTCSEE sequence mutated to nine alanines. LSG1-7Ala-9Ala contains both the seven alanine and nine alanine mutation.

motif. To ask when the ability of LSG1 to interact with VAP evolved in the eukaryotic lineage, we compared LSG1 sequences from species across eukaryotes (Figure 1E). The FFAT-like motif of LSG1 family members, DWQTCSE following an acidic tract, is only recognizable in phylum Chordata, being present in all vertebrates, although somewhat

degenerate in hagfish. The motif also appears to be present, though less well conserved, in LSG1 from Cephalochordates (lancelets) but not present in LSG1 from Urochordata (tunicates) (Figure 1E).

Mapping the LSG1 interaction surface on VAPs

For further evidence that LSG1 binds to VAPs in a manner similar to proteins containing canonical FFAT motifs, we mapped the binding surface of LSG1 on VAP. FFAT motifs bind to a highly conserved, electro-positive face of the major sperm protein (MSP) domain of VAPA with residues K52, T54, K125 (K45, T47, and K118 in VAPB) as critical residues for binding these motifs.[37,38] We used random PCR mutagenesis of VAPA and *in vivo* recombination of the amplicon into the VAPA yeast 2-hybrid construct to generate a library of mutant clones. We then screened these for loss of interaction with LSG1. We identified 24 independent mutants representing 17 different amino acid substitutions at 14 different positions (Figure 2A). Mapping these mutations to the structure of VAPA (Figure 2B and C) revealed two general classes of mutants. One class affected residues within the hydrophobic core of the MSP domain which likely disrupts the overall structure of the domain (Figure 2D red arrow heads). The second class of mutations, involving residues K52, T54, N64, K92, K94, W113, and K125 of VAPA, mapped to the basic surface of the MSP domain that has previously been demonstrated to bind FFAT motifs (Figure 2B to D (blue arrow heads)). Many of these mutations introduced acidic residues which would be expected to reduce affinity for FFAT through electrostatic repulsion of the acidic FFAT motif. Moreover, all but one of these residues have been shown by structural studies to interact directly with the side chains of classical FFAT motifs.[38,39] The one exception, W113, forms a cation-π interaction with K50, which directly interacts with FFAT motifs. We also used AlphaFold Colab[40,41] to predict how the DWQTCS motif interacts with VAPA (Figure 2C). Indeed, the DWQTCS motif is predicted to exactly overlay a canonical FFAT motif, with the tryptophan occupying the position of the first phenylalanine of the canonical FFAT motif and the cysteine buried deep in a pocket on the face of VAPA. The binding of some noncanonical FFAT-like motifs is regulated by phosphorylation of a conserved serine or threonine residue.[42] Notably, T320 within the DWQTCS motif is predicted to lie adjacent to a basic pocket formed by K50 and K52 of VAPA. Phosphorylation of T320 could potentially enhance the interaction between LSG1 and VAPs. The presence of two FFAT-like motifs in human LSG1 (EYED and DWQTCS) raises the interesting possibility that LSG1 could bind two MSP domains simultaneously. As VAPs are known to dimerize,[42] perhaps Lsg1 can bind to both monomers of a VAP dimer.

Amino acids 292–324 of LSG1 are necessary for VAP binding in cells

To verify that the loss of LSG1-VAP interaction identified by yeast 2-hybrid reflects changes in behavior of the protein *in cells*, C-terminal GFP-tagged LSG1 wild-type and mutants were expressed in U2OS Flp-In™ T-REx™ cells and immunoprecipitated with anti-GFP antibody. In addition to WT LSG1 and the loss of VAP interaction mutant LSG1-Δ292–324 (LSG1-ΔVAP-Binding-Region/LSG1-ΔVBR), we also expressed LSG1-D215N, characterized previously as a dominant negative mutant that is likely defective for GTPase activity,[25] and LSG1-D215N in combination with ΔVBR. GFP alone was used as a control.

WT LSG1-GFP but not GFP alone immunoprecipitated VAPA, recapitulating previous results (Figure 3A).[25,28] In contrast, neither LSG1-ΔVBR nor the double mutant LSG1-D215N-ΔVBR immunoprecipitated detectable amounts of VAPA, consistent with our 2-hybrid analysis that LSG1-ΔVBR has lost VAPA interaction (Figure 3A, quantified in Figure 3B, left panel). To ask if there was a correlation between LSG1 binding to VAPA and to ribosomes, we probed for the presence of 60S subunits in the LSG1 IPs using anti-RPL26 (Figure 3A, quantified in Figure 3B). Although we observed a consistent trend that deleting the VAP binding region of LSG1 resulted in increased binding to 60S, when normalized to the LSG1 signal, the difference was not statistically significant (Figure 3B, right panel). Because the LSG1-GFP constructs are expressed at higher levels than endogenous LSG1, it is possible that at endogenous levels of expression, a larger fraction of LSG1-ΔVBR would bind to ribosomes.

Loss of VAP interaction releases LSG1 from the endoplasmic reticulum

GFP-tagged WT LSG1 predominantly localized to the cytoplasm with strong colocalization to the endoplasmic reticulum (ER) although weak signal was also present in the nucleus (Figure 4, left panels). The catalytically inactive LSG1-D215N mutant also localized primarily to the cytoplasm, similar to WT. In contrast, the VAP binding mutant, LSG1-ΔVBR, localized to the cytoplasm, but displayed a distinct loss of colocalization with ER and a correspondingly increased nuclear signal, particularly in nucleoli. We did not examine the colocalization of LSG1 to Cajal bodies reported previously.[24] Similar localization was observed for the double mutant, LSG1-D215N-ΔVBR. To determine if the different cytoplasmic populations of LSG1, ER-bound and cytosolic, were actively shuttling, we used Leptomycin B (LMB) to inhibit CRM1,[43] a cellular export receptor for 60S ribosomal subunits.[16–18] Upon the addition of LMB to cells, WT LSG1 showed a significant redistribution to the nucleus, confirming the shuttling of Lsg1 between the cytoplasm and nucleus reported previously (Figure 4, right panels).[25] However, the ER-associated population of LSG1 remained, suggesting that ER-bound LSG1 does not shuttle or shuttles considerably slower than the non-ER-associated cytosolic pool. In contrast, LSG1-D215N remained predominantly cytosolic in the presence of LMB and continued to colocalize with the ER, suggesting that GTPase activity is necessary for LSG1 shuttling to the nucleus; presumably, the release of LSG1 from 60S subunits requires GTP hydrolysis. In contrast, the VAP binding ΔVBR mutant showed more complete nuclear localization in the presence of LMB than did WT, indicating that loss of VAP binding liberated the ER-bound pool, making it responsive to LMB. Similarly, deleting the VAP binding domain of

A

mutation	frequency
L23P	1
K52E	2
T53I	2
T54A	1
N64D	2
V76D	1
L80Q	1
K92E	1
K94E	1
K94M	1
F95C	1
F95L	2
F95S	2
W113R	2
K125E	1
C128Y	2
M159V	1

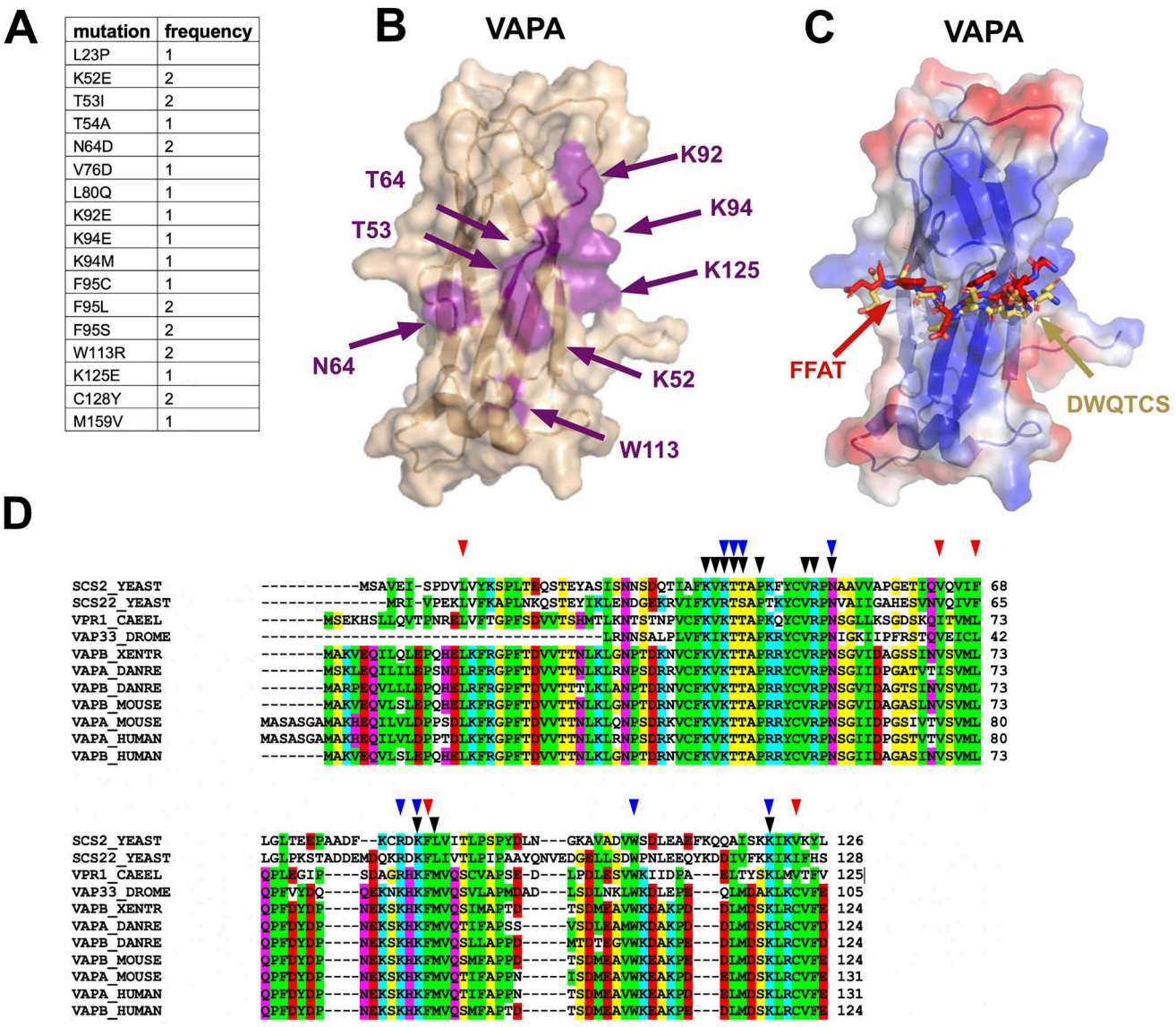

Figure 2. LSG1 binds the same region in VAPs as proteins with canonical FFAT motifs. (A) Mutations in VAPA that resulted in loss of interaction with LSG1 via yeast 2-hybrid. (B) Residues in VAPA identified as important for LSG1 binding (purple) mapped onto the structure of VAPA (PDB 2rr3). (C) FFAT motif of OSBP (red peptide) bound to the MSP domain of VAPA with electrostatic surface potential shown. AlphaFold Colab prediction of the DWQTCS motif of human LSG1 interacting with VAPA (yellow peptide) (D) Alignment of MSP-like domains of various VAP proteins from indicated organisms. Highlighting of residues as in the legend of Figure 2. Black arrowheads indicate residues important for binding FFAT motifs. Colored arrowheads indicate residues that when mutated resulted in loss of LSG1 interaction. Red arrows indicate residues within the hydrophobic core of the MSP domain and blue arrowheads are those that map to the basic surface of the MSP domain that has been demonstrated to bind FFAT motifs.

LSG1 in the D215N mutant led to increased nuclear localization in the presence of LMB. However, a population of the ΔVBR D215N double mutant was retained in the cytosol as a diffuse signal that did not colocalize with ER. Together, these results suggest that there are two distinct cytoplasmic pools of LSG1, one, associated with the ER through interaction with VAPs which effectively does not shuttle, with a second pool not bound to the ER that is presumably associated with 60S subunits and actively shuttles.

LSG1 interaction with VAPs is not required for LSG1-dependent recycling of NMD3

In human cells, as in yeast, the nuclear recycling of the 60S nuclear export adapter NMD3 requires LSG1.[20,23] To determine if LSG1 interaction with VAPs is required for the nuclear recycling of NMD3, we knocked down endogenous LSG1 and rescued with WT LSG1 or LSG1ΔVBR. Targeting the VAP binding region with two siRNAs resulted in efficient knock down of endogenous LSG1 protein (Figure 5A, lanes 1 and 2) whereas control siRNAs did not. Knock down of LSG1 correlated with a change in the localization of NMD3 from primarily nuclear to strongly cytoplasmic, indicating a block in NMD3 recycling (Figure 5B, left panels). Expression of siRNA-resistant LSG1-GFP, restored the ability of NMD3 to shuttle to the nucleus (Figure 5B, middle panels). Importantly, expression of LSG1ΔVBR, which was resistant to knock down by siRNAs targeting the VBR, also restored the nuclear shuttling of NMD3 (Figure 5B, right panels). Because LSG1ΔVBR does not detectably bind to VAP, this result shows that LSG1 binding to VAPs is not necessary for LSG1-dependent recycling of NMD3.

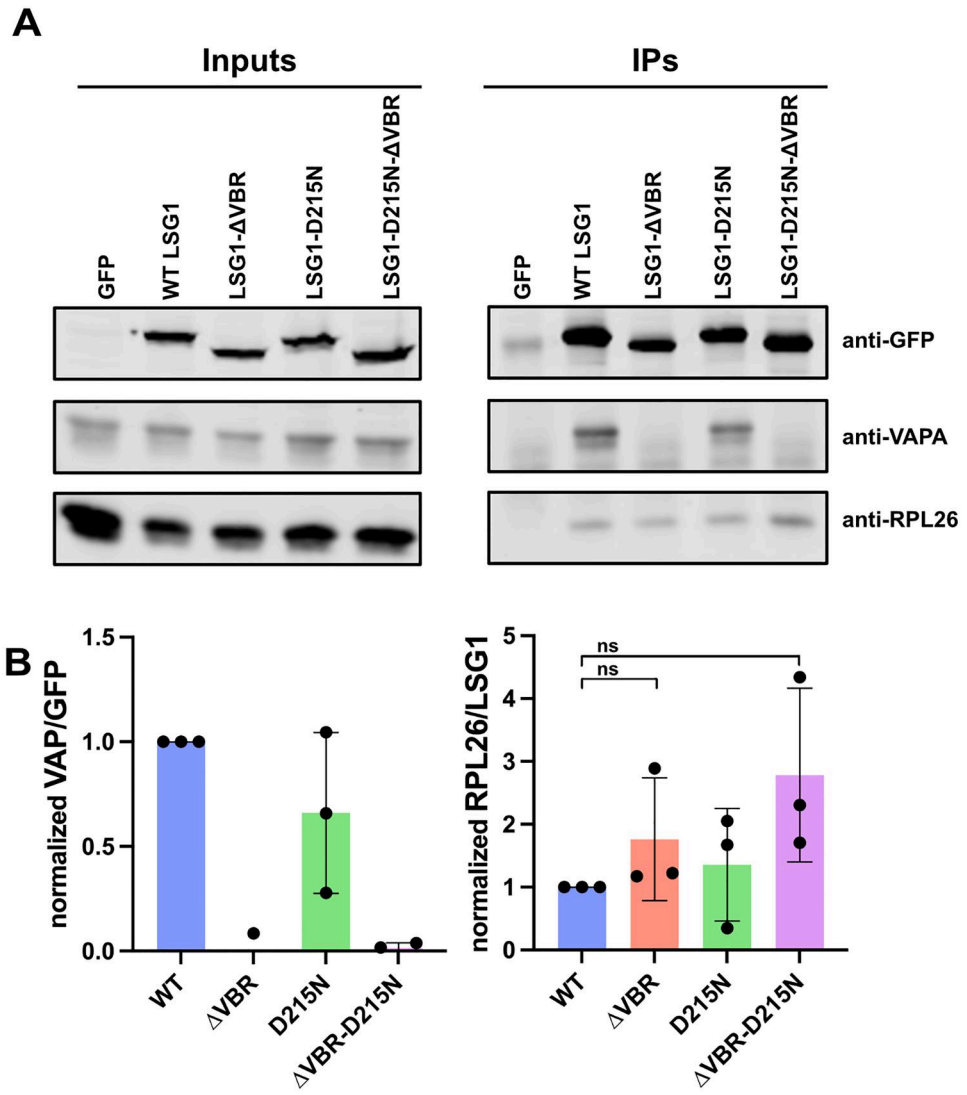

Figure 3. LSG1-ΔVBR mutants lose interaction with VAPA in vivo. (A) Extracts of U2OS cells expressing sfGFP, LSG1(WT)-sfGFP, LSG1-D215N-sfGFP, LSG1-ΔVBR-sfGFP, and LSG1-D215N-ΔVBR-sfGFP were prepared and immunoprecipitated as described in the text. The affinity-purified proteins were separated on a 6–18% SDS-PAGE gel and transferred to nitrocellulose membrane for Western blotting with anti-GFP (LSG1 WT and mutants), anti-VAPA, and anti-RPL26 antibodies. (B) Quantification of VAPA to GFP (left) and RPL26 to GFP signal in IP samples (right), normalized to the ratio for WT. Representative western blots are shown in A. Data in panel B are from biological triplicates. Ns, not statistically significant.

As a complementary means to test the requirement for VAP binding on LSG1 function, we turned to the yeast model. In yeast, the release of Nmd3 is thought to require the GTPase activity of Lsg1; mutation of the P-loop of Lsg1 blocks recycling of Nmd3.[20] Similarly, mutation of the G4 motif of human LSG1 blocks recycling of NMD3 in human cells.[25] We asked if human LSG1 complemented loss of yeast *LSG1* and if human LSG1 lacking the ability to bind yeast VAPs (*SCS2* and *SCS22*) would also complement loss of *LSG1*. Human LSG1 and LSG1ΔVBR were expressed in yeast under control of the strong *TDH3* promoter. Both constructs complemented loss of yeast *LSG1* (Figure 5C), with no discernable difference in the extent of complementation, indicating that VAP interaction is not required for human LSG1 to function in yeast.

As a direct test of the effect of VAPs on LSG1 activity, we asked in VAPs could modulate the GTPase activity of human LSG1 *in vitro*. Although human LSG1 has been reported to display GTPase activity on its own,[24] in yeast, we have shown that the GTPase activity of LSG1 is stimulated by 60S subunits and Nmd3[11]. Indeed, the proper positioning of Switch I of the catalytic center of Lsg1 appears to depend on engagement with ribosomal RNA[11]. Thus, we asked if human LSG1 was similarly activated by 60S and Nmd3 *in vitro* and if this activity was affected by the addition of VAP. Because human LSG1 is functional in yeast, we assayed the GTPase activity of human LSG1 with yeast 60S subunits and yeast Nmd3. Purified human LSG1 was assayed alone or in the presence of 60S or 60S plus Nmd3. Human LSG1 alone displayed modest GTPase activity, which we suspect was due to copurification of a contaminating hydrolytic activity. As a control, we used Lsg1(G440A), which contains a mutation in the G3 motif, necessary for GTP hydrolysis by GTPases. The G440 mutation displayed somewhat reduced GTPase activity when assayed alone. As with yeast Lsg1, human LSG1 GTPase activity was stimulated by the addition of 60S and Nmd3, whereas LSG1(G440A) was not. These results demonstrate that the GTPase activity of human LSG1 is stimulated by the presence

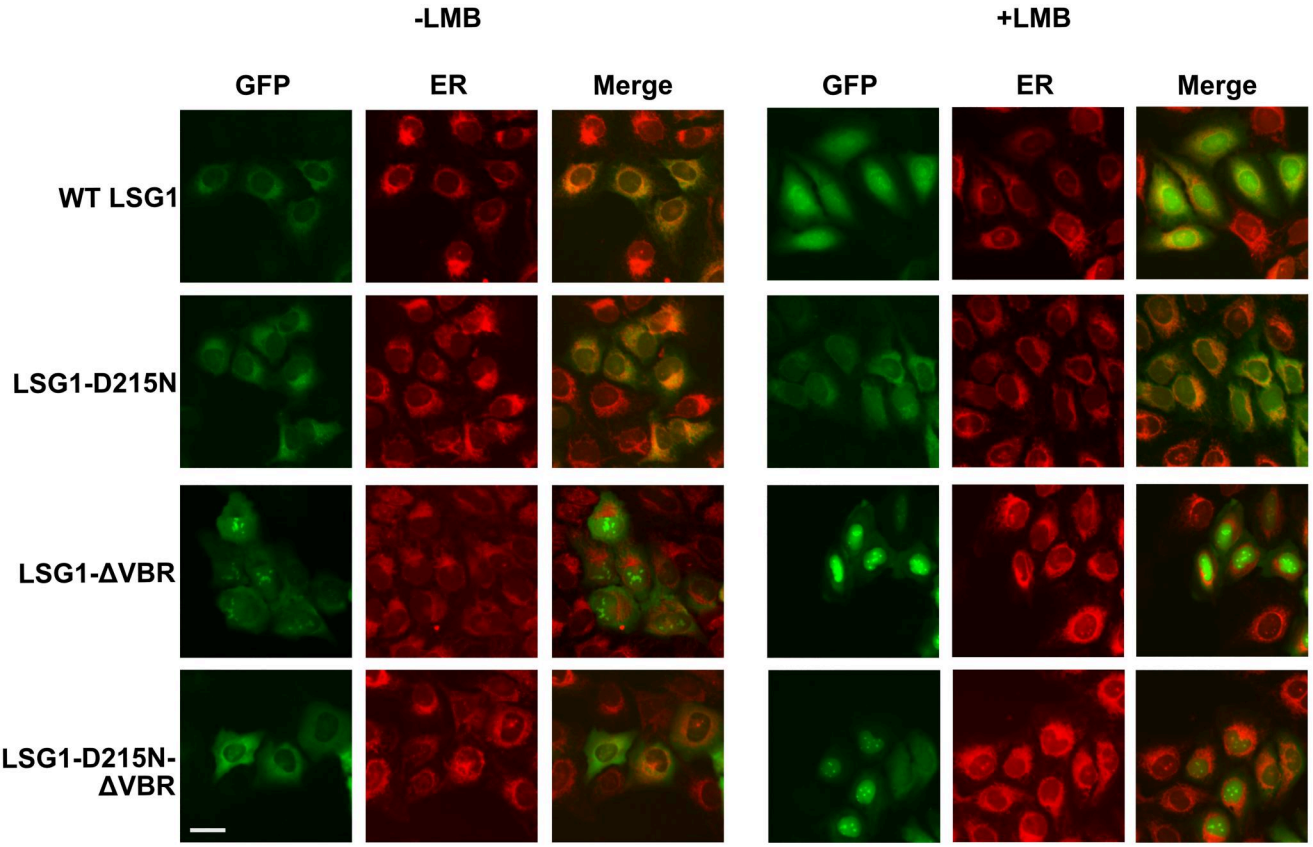

Figure 4. Cellular localization of WT and mutant LSG1. GFP-tagged WT and mutant LSG1 were induced with tetracycline in U2OS cells. Thirty minutes prior to imaging, ER-Tracker™ Red was added to cells. Where indicated, cells were incubated with 100 nM LMB for 5 h prior to imaging. Scale bar: 20 μm.

of 60S and Nmd3. To determine the impact of VAPs on LSG1 GTPase activity, we expressed and purified the soluble MSP domain of human VAPA as a GST fusion. Addition of VAPA to LSG1 in the presence of 60S and Nmd3 had no obvious impact on GTPase activity. This result is consistent with our finding that LSG1 lacking the ability to bind VAPs rescued the NMD3 recycling defect in human cells and rescued Lsg1 function in yeast.

Discussion

The GTPase LSG1 is required for the release of the nuclear export adapter NMD3 from the nascent 60S ribosomal subunit in a late step of ribosome maturation. Although LSG1 acts in the cytoplasm to release NMD3, it is also found in the nucleus, suggesting that it likely shuttles. Here, we have shown that human LSG1 interacts with membrane associated VAP proteins via a noncanonical FFAT-like motif. This interaction tethers a population of LSG1 at the ER and this population is relatively insensitive to the nuclear export inhibitor LMB, suggesting that the ER-associated pool of LSG1 does not actively shuttle. Considering that LSG1 acts late in cytoplasmic maturation, we were particularly interested in the possibility that the interaction between LSG1 and VAPs could be a mechanism to deliver newly made 60S subunits to localized regions within the cytosol.

We mapped the interaction with VAPs to an unstructured region of LSG1 between the circularly permuted G5 and G1 motifs. Structures of LSG1 bound to pre-60S suggest that this region is accessible to the solvent when LSG1 is bound to pre-60S raising the intriguing possibility that the interaction of LSG1 with VAPs could modulate its GTPase activity. However, we found that mutant LSG1 that could not bind to VAPs rescued the ability of LSG1 to promote NMD3 recycling in cells, indicating that this interaction is not required for the known activity of LSG1. We also established that the GTPase activity of human LSG1 is stimulated by the presence of 60S subunits and NMD3, as we have shown previously for the yeast enzyme.[11] However, addition of VAP protein did not affect the 60S- and NMD3-dependent activation of LSG1 *in vitro*, consistent with our observation that the recycling of NMD3 by LSG1 is independent of its interaction with VAPs in cells. Considering this, we think it is unlikely that LSG1 interaction with VAPs would provide a mechanism of depositing newly made ribosome to specific regions of the cell. Rather than directly impinging on LSG1 enzymatic activity, it is possible that tethering LSG1 to VAPs *in vivo* spatially restricts that population of LSG1 in such a way that it cannot engage with ribosomes. In this model, the association of LSG1 with VAPs could be regulated, perhaps in response to particular cellular stresses by phosphorylation of T320 within its noncanonical FFAT-like motif, thereby controlling the availability of LSG1 able to engage with pre-60S subunits.

Our results also raise the possibility that LSG1 may have additional functions in cells beyond its role in the release of NMD3. It has previously been reported that stable knockdown of human LSG1 in fibroblasts results in fragmentation of the tubule structure of the ER and upregulation of cholesterol

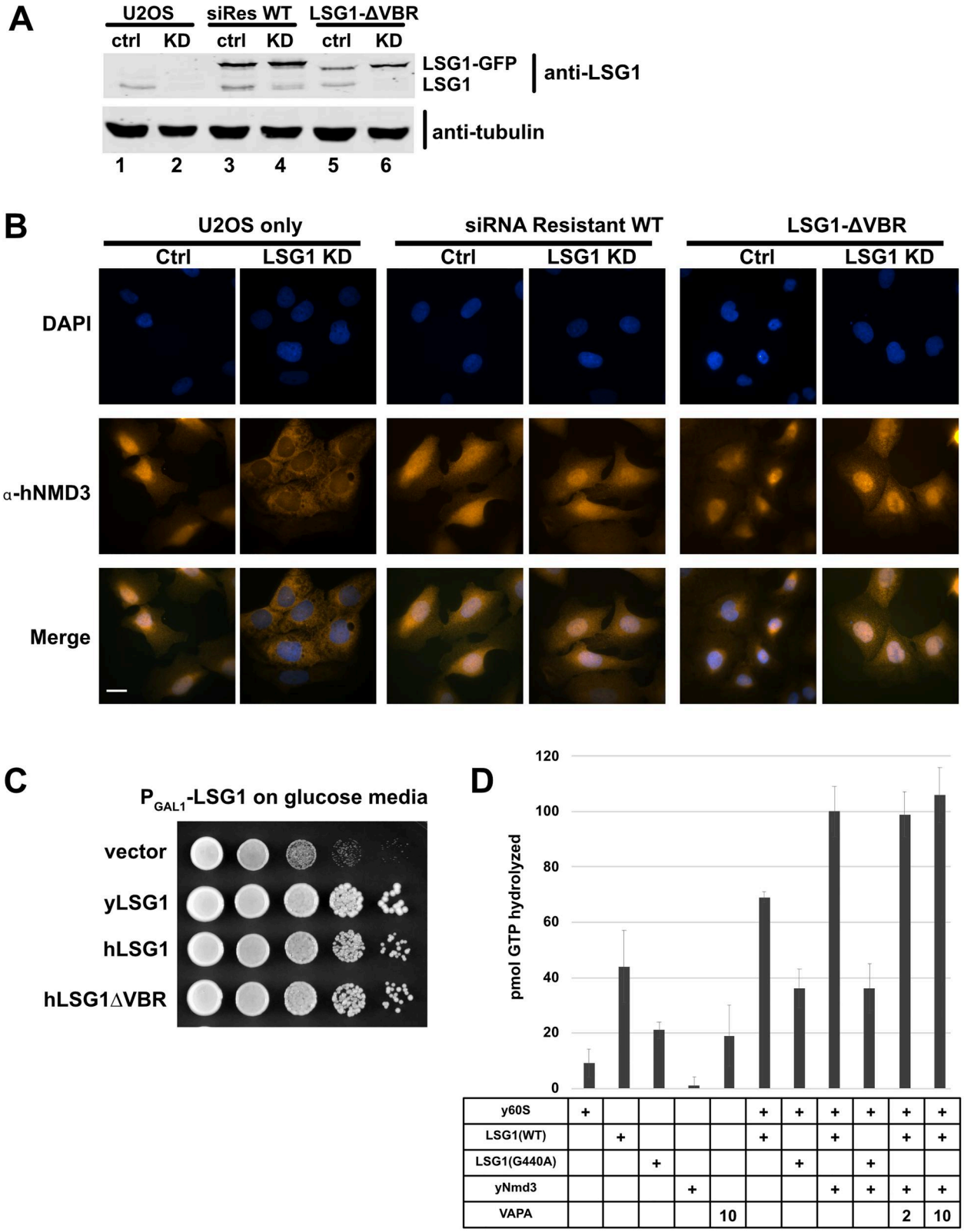

Figure 5. LSG1-ΔVBR rescues NMD3 re-localization upon LSG1 knock down. (A) Western blot showing efficiency of knockdown of endogenous LSG1 and resistance to knockdown of siRNA resistant-WT LSG1 and LSG1-ΔVBR. (B) Indirect immunofluorescence of U2OS cells (left panels) and U2OS cells expressing siRNA resistant-WT LSG1 (middle panels) and LSG1-ΔVBR constructs (right panels) treated with the indicated siRNAs. Immunofluorescence of NMD3 was observed 72 h after introduction of siRNAs against endogenous LSG1. Upper panels: DAPI, middle panels, anti-NMD3 and lower panels, merged. Scale bar: 20 μm. (C) Complementation of repression of yeast LSG1. Ten-fold serial dilutions of cultures of AJY3827 containing empty vector, yeast LSG1, human LSG1 and human LSG1ΔVBR plated on selective media containing glucose. (D) GTPase assays of human LSG1 in the presence and absence of yeast 60S, yeast Nmd3 and VAPA. Mean and standard deviation of biological triplicates are shown.

biosynthetic genes.[23] It is intriguing to note that although yeast Lsg1 does not interact with VAPs, *lsg1Δ/LSG1* heterozygous mutant diploid yeast cells are sensitive to sertraline and other cationic amphiphilic drugs[44] that are thought to perturb the biophysical properties of membranes.[45] Conceivably, haploinsufficiency for *LSG1* in yeast or chronic suppression of LSG1 expression in humans impacts membrane function in a manner that is coupled to sterol biosynthesis.

Materials and methods

Yeast strains

Saccharomyces cerevisiae strains used in this work are listed in Table 1. All yeast were cultured at 30 °C in either YPD (2% peptone, 1% yeast extract, 2% dextrose) or synthetic dropout medium containing 2% dextrose, unless noted otherwise.

Plasmids

Plasmids used in this work are listed in Table 2. For yeast 2-hybrid assays, wild-type *LSG1* was amplified from pAJ3025 using oligos AJO2244 and 2245 and cloned into the GAL4 DNA-binding domain vector pGBKT7 (Clontech) to make pAJ3505. LSG1 deletion and substitution mutations (pAJ3701–3710, 3515–3524, 3534) were derived from pAJ3505 and pAJ3535 was derived from pAJ3522 using inverse PCR with oligos listed in Table 3. Wild-type VAPA was

Table 1. Yeast strains used in this study

Strain	Genotype	Source
PJ69-4alpha	*MATalpha trp1-901 leu2-3, 112 ura3-52 his3-200 gal4? gal80? LYS2::GAL1-HIS3 GAL2-ADE2 met2::GAL7-lacZ*	46
PJ69-4a	*MATa trp1-901 leu2-3, 112 ura3-52 his3-200 gal4? gal80? LYS2::GAL1-HIS3 GAL2-ADE2 met2::GAL7-lacZ*	46
AJY3827	*MATalpha Natr-P_{GAL1}-3xHA-LSG1 his3Δ1 leu2Δ0 ura3Δ0*	11

Table 2. Plasmids used in this study

Plasmid	Description	Source
pACT2	GAL4AD-HA Leu 2u	Clontech
pAJ2228	LSG1 HIS3 CEN Ampr	20
pAJ3025	P_{TDH3}-hLSG1 LEU2 CEN Ampr	This Study
pAJ3026	P_{TDH3}-hLSG1 HIS3 CEN Ampr	This Study
pAJ3447	T7-HIS6-TEV-hLSG1 Kanr	24
pAJ3638	T7-HIS6-TEV-hLSG1(G440A) Kanr	This Study
pAJ3501	VAPA Gateway vector	E Marcotte
pAJ3503	GAL4AD-HA-hVAP-A LEU2 Ampr in pACT2-AD	This Study
pAJ3505	GAL4-BD-mcy-hLSG1 Trp1 Kanr	This Study
pAJ3515	GAL4-BD-myc-hLSG1 Trp1. N-terminal truncation AA 2-93	This Study
pAJ3516	GAL4-BD-myc-hLSG1 TRP1. N-terminal truncation of AA2-253	This Study
pAJ3517	GAL4-BD-myc-hLSG1 TRP1 N-terminal truncation of AA 2-324	This Study
pAJ3518	GAL4-BD-myc-hLSG1 TRP1 N-terminal truncation of AA-2-381	This Study
pAJ3519	GAL4-BD-myc-hLSG1 TRP1 N-terminal truncation of AA 2-556	This Study
pAJ3520	GAL4-BD-myc-hLSG1 TRP1 C-terminal deletion of AA 557-658	This Study
pAJ3521	GAL4-BD-myc-hLSG1 TRP1 C-terminal deletion of AA 382-658	This Study
pAJ3522	GAL4-BD-myc-hLSG1 TRP1 C-terminal deletion of AA 325-658	This Study
pAJ3523	GAL4-BD-myc-hLSG1 TRP1 C-terminal deletion of AA 254-658	This Study
pAJ3524	GAL4-BD-myc-hLSG1 TRP1 C-terminal deletion of AA 94-658	This Study
pAJ3534	GAL4-BD-myc-hLSG1Trp1 Kanr Δaa254-324	This Study
pAJ3535	GAL4-BD-myc-hLSG1Trp1 Kanr with only aa254-324	This Study
pAJ3701	GAL4-BD-myc-hLSG1 Trp1 Kanr aa 292-295AAAA	This Study
pAJ3702	GAL4-BD-myc-hLSG1 Trp1 Kanr aa 296-299AAAA	This Study
pAJ3703	GAL4-BD-myc-hLSG1 Trp1 Kanr aa 300-303AAAA	This Study
pAJ3704	GAL4-BD-myc-hLSG1 Trp1 Kanr aa 304-307AAAA	This Study
pAJ3705	GAL4-BD-myc-hLSG1 Trp1 Kanr aa 308-311AAAA	This Study
pAJ3706	GAL4-BD-myc-hLSG1 Trp1 Kanr aa 312-315AAAA	This Study
pAJ3707	GAL4-BD-myc-hLSG1 Trp1 Kanr aa 316-319AAAA	This Study
pAJ3708	GAL4-BD-myc-hLSG1 Trp1 Kanr aa 320-324AAAAA	This Study
pAJ3709	GAL4-BD-myc-hLSG1 Trp1 Kanr Δaa292-324	This Study
pAJ3710	GAL4-BD-myc-hLSG1 Trp1 Kanr Δaa254-291	This Study
pAJ3718	WT hLSG1-sfGFP in pcDNA5/FRT/TO/intron	This Study
pAJ3719	sfGFP alone in pcDNA5/FRT/TO/intron Ampr	This Study
pAJ3721	hLSG1-D215N-sfGFP in pcDNA5/FRT/TO/intron Ampr	This Study
pAJ3768	Ptac-GST-TEV-VAPA MSP Ampr	This Study
pAJ4144	GAL4-BD-myc-hLSG1-7Ala + 9Ala	This Study
pAJ4260	GAL4-BD-myc-hLSG1-9Ala 2 micron TRP1 Kanr	This Study
pAJ4279	hLSG1 Δaa292-324-sfGFP in pcDNA5/FRT/TO/intron	This Study
pAJ4281	hLSG1-D215N-Δaa292-324-sfGFP in pcDNA5/FRT/TO/intron Ampr	This Study
pAJ4416	pLKO.1—TRC cloning vector with shRNA for hLsg1	This Study
pAJ4421	GAL4-BD-myc-hLSG1-7Ala (EYEDCPE motif mutant)	This Study
pcDNA5/FRT/TO/intron		Addgene
pGBKT7	GAL4-BD-c-myc TRP1 Kanr	Clontech
pLKO.1—TRC	pLKO.1—TRC cloning vector	Addgene
pMD2.G	VSV-G envelope expressing plasmid	Addgene
pMDLg/pRRE	3rd generation lentiviral packaging plasmid; Contains Gag and Pol	Addgene
POG44	Flp-Recombinase Expression Vector	Thermo Scientific
pRSV.Rev	Third generation lentiviral packaging plasmid; Contains Rev	Addgene

Table 3. Oligos used in this study

Oligo	Sequence	Used for
AJO1738	GATACCCCACCAAACCCAAAAAAAGAG	VAPA mutagenesis
AJO1991	GAGTTACTCAAGAACAAGAATTTTCG	VAPA mutagenesis
AJO2244	CGCCCATGGGCCGGAGGAGAGCCCC	pAJ3505
AJO2245	CGCGGATCCTCACATATCCAGGTGCTTGTAGAGTCTACG	pAJ3505
AJO2247	GCGCTCGAGCTAACTGGTGACATTATCTCTGAAGG	pAJ3503
AJO2272	GCGCCCGGGCATGGCGTCCGCCTCAGGGG	pAJ3503
AJO2319	CATGGCCATATGCAGGTCCTCCTC	pAJ3515-pAJ3519, pAJ3522
AJO2320	TTCGAGGAGAGCCAGAGAATTAAG	pAJ3515
AJO2321	GAAGAGGCAAACAGAGATGATAGACAAAGC	pAJ3516, pAJ3522
AJO2322	GACGGTCCCAAGGAAGAGGACTG	pAJ3517, pAJ3534, pAJ3709
AJO2323	GTGAAAGATGGGCAACTTACGGTCGG	pAJ3518
AJO2324	ACTTTTCAGCATCAACACCAGCGAC	pAJ3519
AJO2325	TGAGGATCCGTCGACCTGCAG	pAJ3520-pAJ3524
AJO2326	TACAGGATCTCTTCCAGGAGGAGGATG	pAJ3520
AJO2327	TCTCCCAGTGTGTAGCTCCTTAAAGAGC	pAJ3521
AJO2328	TTCTTCTGAGCACGTCTGCCAGTC	pAJ3522
AJO2329	CTCAGAGTCACCATTCAGGGGAATGG	pAJ3523, pAJ3534, pAJ3710
AJO2330	AGACAGTAGTCCAGTTCTAGCCTCAGC	pAJ3524
AJO2395	GCTGCAGCTGCTGAAAATCCCACAACGG	pAJ3701
AJO2396	AGAATCCCTAGCTGGGAG	pAJ3701
AJO2397	GCAGCTGCCGCAACGGATGAAGATGAC	pAJ3702
AJO2398	ACTAAGTGAAGGAGAATCCC	pAJ3702
AJO2399	GCGGCTGCAGCTGACAGTGAGTATGAGG	pAJ3703
AJO2400	TGTGGGATTTTCACTAAGTGAAGG	pAJ3703
AJO2401	GCCGCTGCGGCTGAGGACTGTCCAGAGG	pAJ3704
AJO2402	ATCTTCATCCGTTGTGGG	pAJ3704
AJO2403	GCGGCCGCTGCAGAGGAGGAGGAAGACG	pAJ3705
AJO2404	ATACTCACTGTCATCTTCATCCG	pAJ3705
AJO2405	GCGGCGGCGGCAGACGACTGGCAGACGTGC	pAJ3706
AJO2406	TGGACAGTCCTCATACTCAC	pAJ3706
AJO2407	GCCGCCGCGGCGACGTGCTCAGAAGAAGACGG	pAJ3707
AJO2408	TTCCTCCTCCTCTGGACAGTCC	pAJ3707
AJO2409	GCGGCCGCAGCAGCAGACGGTCCCAAGGAAGAGG	pAJ3708, pAJ4260
AJO2410	CTGCCAGTCGTCTTCCTCCTCC	pAJ3708
AJO2470	CCTTCACTTAGTGAAAATCCCACAACGG	pAJ3710
AJO2471	AGAATCCCTAGCTGGGAGATGTTCGG	pAJ3709
AJO2764	CGCCGCGGCGGCTTCCTCCTCCTCTGGACAG	pAJ4260
AJO3409	GCGGCCGCTGCCGAGGAGGAAGCCGCCGC	pAJ4144
AJO3410	GGCAGCGGCACTGTCATCTTCATCCGTTGTGG	pAJ4144
AJO3418	TTCCTCCTCGGCAGCGGCCGCGGCAGCGGCACTGTCATCTTCATCCGTTGTGGGATT	pAJ4421
AJO3420	GAAGACGACTGGCAGACGTG	pAJ4421

amplified from pAJ3501 using oligos AJO2272 and 2247 and cloned into pACT2 (Clontech) to make pAJ3503.

For mammalian cell work, sfGFP, LSG1(WT)-sfGFP, LSG1-D215N-sfGFP, LSG1-ΔVBR-sfGFP, LSG1-D215N-sfGFP, were cloned into pcDNA5/FRT/TO/intron to generate vectors (pAJ3719, pAJ3718, pAJ3721, pAJ4279 and pAJ4281, respectively). POG44 is a Flp-Recombinase Expression Vector used in the transfection of U2OS Flp-In™ T-REx™ cells.

Yeast 2-hybrid

WT *LSG1* and mutant plasmids were individually transformed into the MATα haploid yeast strain PJ69-4alpha.[46] The WT VAPA vector (pAJ3503) was transformed into the MATa haploid yeast strain PJ69-4a.[46] Strains were mated and diploids containing AD and BD vectors were selected on Leu-Trp- media. Cells were spotted onto reporter media, as indicated in the figure legends, to assay for interaction.

PCR mutagenesis of VAPA

VAPA was amplified from pAJ3503 using oligos AJO1738 and AJO1991 using Taq DNA polymerase (New England Biolabs) under standard amplification conditions using 20 cycles. Product was gel purified and cotransformed with pAJ3503, previously cut with SmaI and XhoI, into yeast strain AJY2176 also containing pAJ3505. Isolates that showed reduced growth on Leu- Trp- His- media supplemented with 6 mM 3AT were analyzed by western blotting and clones expressing full-length VAPA were sequenced.

Creating stable cell lines of LSG1 WT and mutant using U2OS Flp-In™ T-REx™ cells

U2OS Flp-In™ T-REx™ cells were transfected using Lipofectamine™ 3000 Transfection Reagent (Thermo Fisher #L3000015) with 0.5 μg of the insert plasmid and 4.5 μg of the pOG44 plasmid following the manufacture's guidelines. Cells with integrated LSG1 constructs were selected by addition of 100 μg/mL Hygromycin to the media.

LSG1 siRNA knockdown

siRNAs used in this study are listed in Table 4. U2OS cells stably expressing an siRNA resistant WT LSG1 or LSG1-ΔVBR were transfected with two siRNAs that target the VBR of endogenous LSG1 using Optimem and Lipofectamine RNAiMAX (Thermo Fisher #13778075) at the time of seeding.

Table 4. siRNAs used in this study

siRNAs	Sequence	Origin
ON-TARGETplus Nontargeting Control Pool		Horizon Discovery
VBR_1_sense	GAUGAAGAUGACAGUGAGUAU[dT][dT]	This study
VBR_1_antisense	[Phos]AUACUCACUGUCAUCUUCAUC[dT][dT]	This study
VBR_2_sense	GACGACUGGCAGACGUGCU[dT][dT]	This study
VBR_2_antisense	[Phos]AGCACGUCUGCCAGUCGUC[dT][dT]	This study

Twenty milliliters of cells per condition were seeded at 1×10^5 cells/mL and incubated for 72 h at 37 °C post-transfection prior to harvest.

Live cell imaging

Stable U2OS cell lines expressing LSG1 constructs were induced with 100 μg/mL tetracycline at least 19 h prior to imaging. For cells treated with LMB, 100 nM LMB was added to cells 14 h postinduction with tetracycline. Cells were incubated at 37 °C for 5 h prior to imaging. Thirty minutes prior to imaging, complete medium was replaced with Hank's Balanced Salt Solution (HBSS) with calcium and magnesium (Gibco #14025-092) and 1 μM ER-Tracker™ Red (Thermo Fisher #E34250). Cells were incubated with dye for 30 min at 37 °C. Immediately prior to imaging, the HBSS staining solution was replaced with HBSS alone. Fluorescent signal was captured on a Nikon Eclipse E800 microscope fitted with a Plan Apo 100X/1.4-nimerical-aperature objective and a sCMOS pco.edge camera controlled by NIS-Elements AR 5.11.01 software. Photos were processed with Affinity Designer.

Immunofluorescence

Cells seeded on coverslips at 10^4 cells/mL were fixed with 2% formaldehyde added directly to the growth media and incubated for 15 min on a rocker at room temp. Cells were washed three times with PBS at RT for 5 min each on a rocker. Cells were blocked/permeabilized with 1 mL of PBS, 3% BSA, and 0.6% Triton X-100 for 15 min at RT. Cells were then incubated with 100 μL of PBS, 3% BSA containing the primary antibody (Proteintech NMD3 polyclonal antibody 16060-1-AP) at 1:1000 dilution overnight at 4 °C. Cells were washed three times with PBS at RT for 5 min each on a rocker. Cells were then incubated with 100 μL of (PBS, 3% BSA) containing the secondary antibody (goat anti-rabbit antibody–Alexafluor 555 (ThermoFisher) at 1:1000 dilution and 1 ug/mL DAPI for 1 h at RT in the dark. Cells were washed four times with PBS at RT for 5 min each on a rocker. Coverslips with fixed cells were mounted on glass slides with 3 μL of Vectashield (Vector Laboratories) and sealed with nail varnish. Imaging was done as described above under Live Cell Imaging.

Immunoprecipitation

LSG1 cell lines were harvested at about at 3×10^5 cells/mL in 100 mL total volume. Approximately 12 h prior to harvest, expression was induced with 100 μg/mL tetracycline. Cells were washed with PBS and then harvested via trypsinization. Cells were spun down at 450 × *g* for 1 min at 4 °C. Cells were then washed twice with ice cold wash buffer (50 mM KCl, 20 mM Tris HCl pH 7.4, 2 mM $MgCl_2$, 1 μM pepstatin, 1 μM leupeptin, 1 mM PMSF, and 5 mM BME). Cell pellets were resuspended in 750 μL of IP buffer (wash buffer plus 0.5% NP40) and triturated through a 23 gauge needle approximately five times followed by incubation on ice for 15 min. Lysates were clarified at 18,000 × *g* at 4 °C, the supernatant was removed and 2 μL of anti-GFP antibody was added to each sample. Tubes were rotated at 4 °C for 30 min. 0.9 mg of protein G Dynabeads (Invitrogen), pre-equilibrated in IP buffer, was added to each lysate and anti-GFP mixture. Samples were rotated at 4 °C for an additional 30 min. Dynabeads were separated from supernatant on a magnetic rack. Beads were washed three times for 5 min using 1 mL IP buffer at 4 °C and then resuspended in 50 μL of 1× Laemmeli sample buffer with heating. Input and IP samples were loaded onto a 6–18% SDS-PAGE gradient gel.

Western blots

Proteins samples for western blotting were processed as described above. Membranes were incubated with primary antibody under the following conditions: 1:10,000 dilution of anti-RPL26 (Bethel A300-686A) for 1 h at room temperature, 1:10,000 dilution of anti-tubulin (Millipore Sigma CP06-100UG) for 1 h at room temperature, 1:10,000 dilution of anti-GFP for 1 h at room temperature, 1:5000 anti-LSG1 (Proteintech 17750) over night at 4 C, or 1:5000 anti-VAPA (W. Trimble) over night at 4 °C. Secondary antibodies used were goat anti-rabbit antibody–IRDye 680RD (Li-Cor Biosciences) and goat anti-mouse antibody–IRDye 800CW (Li-Cor Biosciences). Western blots were imaged with an Odyssey CLx infrared imaging system (Li-Cor Biosciences) using Image Studio (Li-Cor Biosciences).

Protein purification

LSG1: Wild-type human LSG1 and LSG1(G440A) were expressed from pAJ3447 and pAJ3638, respectively, in codon + BL21(DE3) cells (Agilent) for 4 h at 30 °C with the addition of 1 mM IPTG. All subsequent steps were performed at 0–4 °C. Cells were resuspended in extraction buffer (40 mM Tris-HCl pH 8, 500 mM NaCl, 10% glycerol, 5 mM BME, 1 mM PMSF and 1 μM each leupeptin and pepstatin) supplemented with 10 mM imidazole. Cells were disrupted by sonication and the extract was clarified by centrifugation at 25,000 *g* for 20 min. Clarified extract was bound to Ni-NTA resin (Invitrogen). Resin was washed with extraction buffer supplemented 20 mM imidazole and protein was eluted with extraction buffer supplemented with 250 mM imidazole. Peak

fractions were diluted to 50 mM NaCl in S buffer (40 mM Tris-HCl pH 8, 10% glycerol and 5 mM BME) and applied to a Source 15S column which was developed with a NaCl gradient from 50 to 1000 mM NaCl in S buffer. Peak fractions were concentrated in a 30,000 mwco filter, flash frozen and stored at −80 °C.

VAPA: The MSP domain of VAPA was expressed and purified as a fusion to GST. Codon + BL21 (DE3) cells (Agilent) containing pAJ3768 were grown in LB medium containing ampicillin and chloramphenicol. At OD600 = 0.4 expression was induced with 1 mM IPTG for 4 h at 30 °C. Cells were washed and resuspended in cold high salt lysis buffer (40 mM Tris-HCL, pH8.0, 500 mM NaCl, 10% glycerol, 5 mM BME, 1 mM PMSF and 1 uM each leupeptin and pepstatin). All subsequent steps were performed at 0–4 °C. Cells were disrupted by sonication and the extract was clarified by centrifugation at 25,000 *g* for 20 min. Clarified extract was bound to glutathione-sepharose beads in batch. The beads were transferred to a column and washed extensively with low salt buffer (40 mM Tris-HCL, pH8.0, 50 mM NaCl, 10% glycerol, 1 mM PMSF and 1 μM each leupeptin and pepstatin). Protein was eluted in low salt buffer containing 50 μM glutathione. Peak fractions were pooled and dialyzed against 50 mM Tris-HCl, pH 8.0, 50 mM NaCl and 5% glycerol, flash frozen and stored at −80 °C.

Nmd3 and 60S subunits: Yeast Nmd3 and 60S subunits were prepared as previously described.[11] All protein concentrations were determined using a Qubit4 (Invitrogen) and 60S subunits were quantified by A260.

GTPase assays

Reactions (25 μL) were set up on ice in reaction buffer (20 mM HEPES-KOH pH 7.5, 50 mM KCl, 2 mM Mg acetate, 1 mM DTT). Reactions were initiated by the addition of GTP to a final concentration of 40 μM containing a trace amount of [alpha-^{32}P]-GTP (Perkin Elmer) and incubated for 20 min at 30 °C. Reactions were quenched on ice with 6.25 μL 0.5 M EDTA and 1 μL of each reaction was spotted onto a PEI-cellulose thin layer chromatography plate (Sigma-Aldrich) and developed in 0.8 M CH_3COOH and 0.8 M lithium chloride. GTP and GDP were imaged with a storage phosphor screen on a Typhoon Phosphoimager. Data was analyzed using ImageJ software (NIH). All samples were corrected for non-enzymatic background hydrolysis.

Acknowledgments

We thank E. Marcotte for pAJ3501, pAJ3025 and pAJ3026, E. Reynaud for pAJ3447, M. Rout for anti-GFP antibody, and W. Trimble for anti-VAPA antibody.

Disclosure statement

No potential conflict of interest was reported by the authors.

Funding

This work was supported by grant R35-GM127127 to AWJ and R01-GM127802 to BX.

ORCID

Sharmishtha Musalgaonkar http://orcid.org/0000-0003-4177-9308
Blerta Xhemalce http://orcid.org/0000-0002-0517-9607
Arlen W. Johnson http://orcid.org/0000-0002-4742-085X

Data availability statement

No large datasets requiring deposition in a database were generated in this study.

References

1. Klinge S, Woolford JL. Ribosome assembly coming into focus. Nat Rev Mol Cell Biol. 2019;20:116–131. doi:10.1038/s41580-018-0078-y.
2. Peña C, Hurt E, Panse VG. Eukaryotic ribosome assembly, transport and quality control. Nat Struct Mol Biol. 2017;24:689–699. doi:10.1038/nsmb.3454.
3. Dörner K, Ruggeri C, Zemp I, Kutay U. Ribosome biogenesis factors—from names to functions. EMBO J. 2023;42:e112699. doi:10.15252/embj.2022112699.
4. Baßler J, Hurt E. Eukaryotic ribosome assembly. Annu Rev Biochem. 2019;88:281–306. doi:10.1146/annurev-biochem-013118.
5. Kargas V, Castro-Hartmann P, Escudero-Urquijo N, Dent K, Hilcenko C, Sailer C, Zisser G, Marques-Carvalho MJ, Pellegrino S, Wawiórka L, et al. Mechanism of completion of peptidyltransferase centre assembly in eukaryotes. Elife. 2019;8:1–26. doi:10.7554/eLife.44904.
6. Prattes M, Grishkovskaya I, Hodirnau V-V, Hetzmannseder C, Zisser G, Sailer C, Kargas V, Loibl M, Gerhalter M, Kofler L, et al. Visualizing maturation factor extraction from the nascent ribosome by the AAA-ATPase Drg1. Nat Struct Mol Biol. 2022;29:942–953. doi:10.1038/s41594-022-00832-5.
7. Liang X, Zuo M, Zhang Y, Li N, Ma C, Dong M, Gao N. Structural snapshots of human pre-60S ribosomal particles before and after nuclear export. Nat Commun. 2020;11:3542. http://www.nature.com/articles/s41467-020-17237-x. doi:10.1038/s41467-020-17237-x.
8. Li Z, Chen S, Zhao L, Huang G, Xu H, Yang X, Wang P, Gao N, Sui SF. Nuclear export of pre-60S particles through the nuclear pore complex. Nature. 2023;618:411–418. doi:10.1038/s41586-023-06128-y.
9. Ma C, Wu S, Li N, Chen Y, Yan K, Li Z, Zheng L, Lei J, Woolford JL, Jr, Gao N. Structural snapshot of cytoplasmic pre-60S ribosomal particles bound by Nmd3, Lsg1, Tif6 and Reh1. Nat Struct Mol Biol. 2017;24:214–220. doi:10.1038/nsmb.3364.
10. Zhou Y, Musalgaonkar S, Johnson AW, Taylor DW. Tightly-orchestrated rearrangements govern catalytic center assembly of the ribosome. Nat Commun. 2019;10:958. doi:10.1038/s41467-019-08880-0.
11. Malyutin AG, Musalgaonkar S, Patchett S, Frank J, Johnson AW. Nmd3 is a structural mimic of eIF5A, and activates the cpGTPase Lsg1 during 60S ribosome biogenesis. EMBO J. 2017;36:854–868. doi:10.15252/embj.201696012.
12. Panse VG, Johnson AW. Maturation of eukaryotic ribosomes: acquisition of functionality. Trends Biochem Sci. 2010;35:260–266. doi:10.1016/j.tibs.2010.01.001.
13. Kemmler S, Occhipinti L, Veisu M, Panse VG. Yvh1 is required for a late maturation step in the 60S biogenesis pathway. J Cell Biol. 2009;186:863–880. https://rupress.org/jcb/article/186/6/863/35660/Yvh1-is-required-for-a-late-maturation-step-in-the. doi:10.1083/jcb.200904111.
14. Lo K-Y, Li Z, Wang F, Marcotte EM, Johnson AW. Ribosome stalk assembly requires the dual-specificity phosphatase Yvh1 for the

exchange of Mrt4 with P0. J Cell Biol. 2009;186:849–862. doi:10.1083/jcb.200904110.
15. Espinar-Marchena FJ, Babiano R, Cruz J. Placeholder factors in ribosome biogenesis: please, pave my way. Microb Cell. 2017;4:144–168. doi:10.15698/mic2017.05.572.
16. Ho JH-N, Kallstrom G, Johnson AW. Nmd3p is a Crm1p-dependent adapter protein for nuclear export of the large ribosomal subunit. J Cell Biol. 2000;151:1057–1066. https://rupress.org/jcb/article/151/5/1057/45793/Nmd3p-Is-a-Crm1p-Dependent-Adapter-Protein-for. doi:10.1083/jcb.151.5.1057.
17. Thomas F, Kutay U. Biogenesis and nuclear export of ribosomal subunits in higher eukaryotes depend on the CRM1 export pathway. J Cell Sci. 2003;116:2409–2419. doi:10.1242/jcs.00464.
18. Trotta CR, Lund E, Kahan L, Johnson AW, Dahlberg JE. Coordinated nuclear export of 60s ribosomal subunits and NMD3 in vertebrates. EMBO J. 2003;22:2841–2851. doi:10.1093/emboj/cdg249.
19. Lo K-Y, Li Z, Bussiere C, Bresson S, Marcotte EM, Johnson AW. Defining the pathway of cytoplasmic maturation of the 60S ribosomal subunit. Mol Cell. 2010;39:196–208. doi:10.1016/j.molcel.2010.06.018.
20. Hedges J, West M, Johnson AW. Release of the export adapter, Nmd3p, from the 60S ribosomal subunit requires Rpl10p and the cytoplasmic GTPase Lsg1p. EMBO J. 2005;24:567–579. doi:10.1038/sj.emboj.7600547.
21. Kallstrom G, Hedges J, Johnson A. The putative GTPases Nog1p and Lsg1p are required for 60S ribosomal subunit biogenesis and are localized to the nucleus and cytoplasm, respectively. Mol Cell Biol. 2003;23:4344–4355. doi:10.1128/mcb.23.12.4344-4355.2003.
22. Anand B, Verma SK, Prakash B. Structural stabilization of GTP-binding domains in circularly permuted GTPases: implications for RNA binding. Nucleic Acids Res. 2006;34:2196–2205. doi:10.1093/nar/gkl178.
23. Pantazi A, Quintanilla A, Hari P, Tarrats N, Parasyraki E, Dix FL, Patel J, Chandra T, Carlos Acosta J, Finch AJ. Inhibition of the 60S ribosome biogenesis GTPase LSG1 causes endoplasmic reticular disruption and cellular senescence. Aging Cell. 2018;18:e12981. doi:10.1101/463851.
24. Reynaud EG, Andrade MA, Bonneau F, Ly TB, Knop M, Scheffzek K, Pepperkok R. Human Lsg1 defines a family of essential GTPases that correlates with the evolution of compartmentalization. BMC Biol. 2005;3:21. doi:10.1186/1741-7007-3-21.
25. Wyler E. Tandem affinity purification combined with inducible shRNA expression as a tool to study the maturation of macromolecular assemblies. Zurich (Switzerland): ETH; 2010. doi:10.1261/rna.2325911.
26. Cabukusta B, Berlin I, Van Elsland DM, Janssen GMC, Van Veelen PA, Neefjes J, Forkink I, Spits M, De Jong AWM, Akkermans JJLL, et al. Human VAPome analysis reveals MOSPD1 and MOSPD3 as membrane contact site proteins interacting with FFAT-related FFNT motifs. Cell Rep. 2020;33:108475. doi:10.1016/j.celrep.2020.108475.
27. James C, Kehlenbach RH. The interactome of the VAP family of proteins: an overview. Cells. 2021;10:1780. doi:10.3390/cells10071780.
28. Huttlin EL, Ting L, Bruckner RJ, Gebreab F, Gygi MP, Szpyt J, Tam S, Zarraga G, Colby G, Baltier K, et al. The BioPlex network: a systematic exploration of the human interactome. Cell. 2015;162:425–440. doi:10.1016/j.cell.2015.06.043.
29. Oughtred R, Stark C, Breitkreutz B-J, Rust J, Boucher L, Chang C, Kolas N, O'Donnell L, Leung G, McAdam R, et al. The BioGRID interaction database: 2019 update. Nucleic Acids Res. 2019;47:D529–D541. doi:10.1093/nar/gky1079.
30. Gavin A-C, Bösche M, Krause R, Grandi P, Marzioch M, Bauer A, Schultz J, Rick JM, Michon A-M, Cruciat C-M, et al. Functional organization of the yeast proteome by systematic analysis of protein complexes. Nature. 2002;415:141–147. https://www.nature.com/articles/415141a. doi:10.1038/415141a.
31. Lev S, Ben HD, Peretti D, Dahan N. The VAP protein family: from cellular functions to motor neuron disease. Trends Cell Biol. 2008;18:282–290. doi:10.1016/J.TCB.2008.03.006.
32. Murphy SE, Levine TP. VAP, a versatile access point for the endoplasmic reticulum: review and analysis of FFAT-like motifs in the VAPome. Biochim Biophys Acta. 2016;1861:952–961. doi:10.1016/j.bbalip.2016.02.009.
33. Loewen CJR, Roy A, Levine TP. A conserved ER targeting motif in three families of lipid binding proteins and in Opi1p binds VAP. EMBO J. 2003;22:2025–2035. doi:10.1093/EMBOJ/CDG201.
34. Wyles JP, McMaster CR, Ridgway ND. Vesicle-associated membrane protein-associated protein-A (VAP-A) interacts with the oxysterol-binding protein to modify export from the endoplasmic reticulum. J Biol Chem. 2002;277:29908–29918. doi:10.1074/jbc.M201191200.
35. Leipe DD, Wolf YI, Koonin EV, Aravind L. Classification and evolution of P-loop GTPases and related ATPases. J Mol Biol. 2002;317:41–72. https://linkinghub.elsevier.com/retrieve/pii/S0022283601953781. doi:10.1006/jmbi.2001.5378.
36. Slee JA, Levine TP. Systematic prediction of FFAT motifs across eukaryote proteomes identifies nucleolar and eisosome proteins with the predicted capacity to form bridges to the endoplasmic reticulum. Contact (Thousand Oaks). 2019;2:1–21. https://us.sagepub.com/en-us/nam/open-access-at-sage. doi:10.1177/2515256419883136.
37. Loewen CJR, Levine TP. A highly conserved binding site in vesicle-associated membrane protein-associated protein (VAP) for the FFAT motif of lipid-binding proteins. J Biol Chem. 2005;280:14097–14104. doi:10.1074/jbc.M500147200.
38. Kaiser SE, Brickner JH, Reilein AR, Fenn TD, Walter P, Brunger AT. Structural basis of FFAT motif-mediated ER targeting. Structure. 2005;13:1035–1045. doi:10.1016/j.str.2005.04.010.
39. Furuita K, Jee J, Fukada H, Mishima M, Kojima C. Electrostatic interaction between oxysterol-binding protein and VAMP-associated protein A revealed by NMR and mutagenesis studies. J Biol Chem. 2010;285:12961–12970. doi:10.1074/jbc.M109.082602.
40. Jumper J, Evans R, Pritzel A, Green T, Figurnov M, Ronneberger O, Tunyasuvunakool K, Bates R, Žídek A, Potapenko A, et al. Highly accurate protein structure prediction with AlphaFold. Nature. 2021;596:583–589. doi:10.1038/s41586-021-03819-2.
41. Mirdita M, Ovchinnikov S, Steinegger M, Schütze K, Moriwaki Y, Heo L. ColabFold: making protein folding accessible to all. Nat Methods. 2022;19:679–682. doi:10.1038/s41592-022-01488-1.
42. Di Mattia T, Martinet A, Ikhlef S, McEwen AG, Nominé Y, Wendling C, Poussin-Courmontagne P, Voilquin L, Eberling P, Ruffenach F, et al. FFAT motif phosphorylation controls formation and lipid transfer function of inter-organelle contacts. EMBO J. 2020;39:e104369. doi:10.15252/embj.2019104369.
43. Kudo N, Matsumori N, Taoka H, Fujiwara D, Schreiner EP, Wolff B, Yoshida M, Horinouchi S. Leptomycin B inactivates CRM1/exportin 1 by covalent modification at a cysteine residue in the central conserved region. Proc Natl Acad Sci USA. 1999;96:9112–9117. doi:10.1073/pnas.96.16.9112.
44. Lee AY, St Onge RP, Proctor MJ, Wallace IM, Nile AH, Spagnuolo PA, Jitkova Y, Gronda M, Wu Y, Kim MK, et al. Mapping the cellular response to small molecules using chemogenomic fitness signatures. Science. 2014;344:208–211. http://chemogenomics.pharmacy.ubc.ca/HIPHOP/.TherawmicroarraydataarearchivedintheArrayExpressdatabase. doi:10.1126/science.1250217.
45. Chen J, Korostyshevsky D, Lee S, Perlstein EO. Accumulation of an antidepressant in vesiculogenic membranes of yeast cells triggers autophagy. PLoS One. 2012;7:e34024. doi:10.1371/journal.pone.0034024.
46. James P, Halladay J, Craig EA. Genomic libraries and a host strain designed for highly efficient two-hybrid selection in yeast. Genetics. 1996;144:1425–1436. doi:10.1093/genetics/144.4.1425.